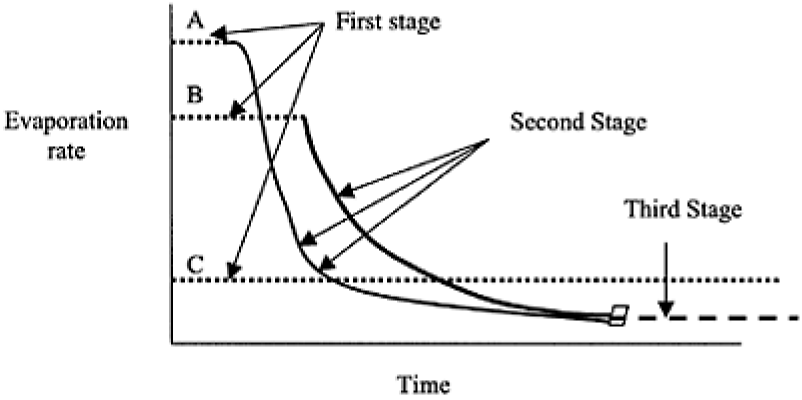

FIGURE 15.4 Stages of evaporation from a soil during steady atmospheric condition.

conductivity. This results in a decrease in evaporation rate with respect to time. The length of time the initial stage of drying can go on depends on the evaporativity. A low evaporativity will increase the duration of first stage of drying.

15.4.3 Evaporation from Layered Soils

Steady evaporation from layered soils can be determined similar to that from a homogeneous profile. Willis (1960) carried out the analysis by assuming that steady flow through layered profile depends upon the transmission property of soil. He further assigned that the suction or matric potential is continuous through the entire soil profile, although water content and conductivity are discontinuous using the relationship between $K(\Phi_m)$ and Φ_m [Eq. (15.7)] (Gardner, 1958) and assuming that each layer is internally homogeneous, he proposed the following relationship:

$$\int_0^{d_2} \mathrm{d}z + \int_{d_2}^{d_1+d_2} \mathrm{d}z = \int_{\Phi_{m0}}^{\Phi_{mL}} \frac{\mathrm{d}\Phi_m}{1+e/K_1(\Phi_m)} + \int_{\Phi_{mL}}^{\Phi_{m(L+d)}} \frac{\mathrm{d}\Phi_m}{1+e/K_2(\Phi_m)} \tag{15.11}$$

where d_1 and d_2 are the thickness of top and bottom layers respectively. Eq. (15.11) relates depth of water table to suction for a given evaporation rate. The limiting evaporation rate for a known water table depth can be calculated from above equation by assuming the suction (Φ_m) to

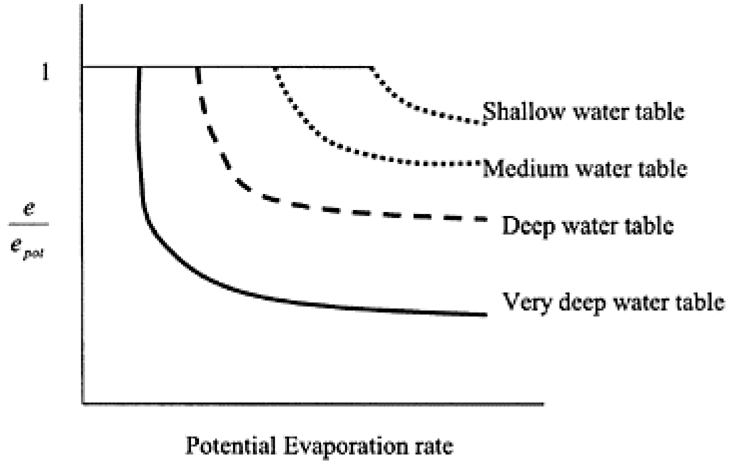

FIGURE 15.5 Dependence of relative evaporation rates, *(e/e*$_{pot}$*)* upon potential evaporation rate (evaporativity, *e*$_{pot}$) for a clay soil. Numbers labeling the curve indicate the depth to water table (cm). (Modified from Ripple et al., 1972.)

be infinite at soil surface. Ripple et al. (1972) proposed a graphical method to measure the steady state evaporation from a multilayer soil profile. They included both the soil properties (i.e., water retention and transmission, vapor flow, depth of water table) and the meteorological factors (i.e., humidity, air temperature, and wind velocity) (Figs. 15.5 and 15.6).

15.4.4 Mathematical Modeling of Stages of Drying

The difference in suction at soil surface and a location with the soil body supplying water is much higher as compared to the depth of soil involved in the process of drying. Therefore, gravity effects are generally neglected for evaporation calculations. Most analysis is based on soil water content and the hydraulic diffusivity relationship. The first and second stages of drying depend upon the hydraulic diffusivity. In order to derive approximate description of drying in the first stage (Fig. 15.6), Gardner (1959) assumed that the evaporation rate from a soil profile of depth *(L)* could be expressed as

$$e = -L\frac{\partial\theta}{\partial t} \tag{15.12}$$

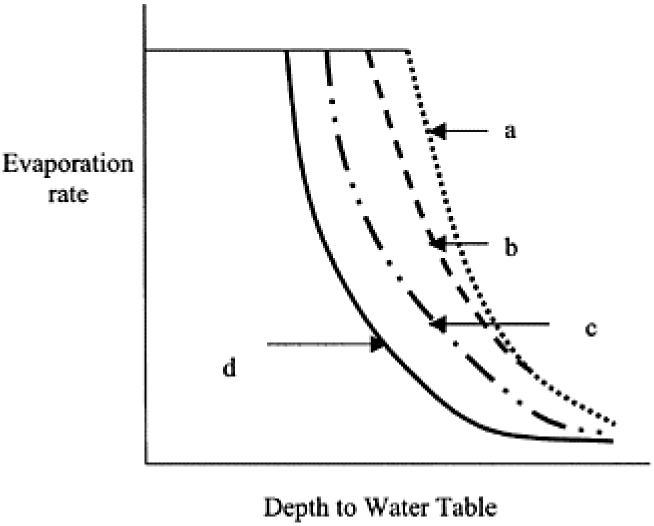

FIGURE 15.6 Effect of horizonation and water table depth on the evaporation rate: (a) limiting curve for soil water evaporation from for homogeneous soil; (b) a two-layer soil with the upper layer thickness of 3 cm; (c) thickness 10 cm; (d) a three-layer soil with thickness of intermediate and uppermost layers equal to 10 cm each. (Modified from Ripple et al., 1972.)

if the soil water diffusivity ($D(\theta)$) can be expressed by the following relationship (Gardner and Mayhugh, 1958)

$$D(\theta)=D(\theta)_0\exp[\beta(\theta-\theta_0)] \tag{15.13}$$

where $D(\theta)_0$ correspond to θ_0 and β ranges from 1 to 30. Gardner (1959) combined Eqs. (15.12) and (15.13) and after further approximation proposed that the total water content of soil profile can be approximated by the following relationship:

$$W=\frac{\beta W}{L} \tag{15.14}$$

and

$$D(\theta)=\frac{2D(\theta)_0}{e_{\text{pot}}\beta L} \tag{15.15}$$

where *W* is the water storage in the entire soil profile at the end of first stage $t=t_1$.

$$W=\int_0^L \theta(z,t_1)\mathrm{d}z \tag{15.16}$$

Gardner and Hillel (1962) also assumed that the evaporation rate from soil profile is given by Eq. (15.12) and the flow equation as follows

$$-\frac{e}{L}=\frac{\partial\theta}{\partial t}=\frac{\partial}{\partial z}\left(D\frac{\partial\theta}{\partial z}\right) \tag{15.17}$$

where z is the height above the bottom of soil profile. Eq. (15.17) was integrated once. The constant of integration was assumed zero since flow through bottom of the soil profile ($z=0$) is zero. Assuming *D* can be represented by Eq. (15.13), Gardner and Hillel (1962) found that actual evaporation rate ceases to be equal to potential rate when at z=L, $\theta=\theta_0$. They proposed the following equation for total water content *(W)* of profile.

$$W=\frac{L}{\beta}\ln\left(1+\frac{e\beta L}{2D_0}\right) \tag{5.18}$$

For a long soil column dependence of *e* on *t* is only approximately valid. For a soil column of finite length *(L)*, Gardner and Hillel (1962) proposed the following relationship to calculate evaporation during second stage (Fig. 15.5).

$$e=-\frac{\mathrm{d}W}{\mathrm{d}t}=D(\bar{\theta})\frac{W\pi^2}{4L^2} \tag{15.19}$$

where $\bar{\theta}$ is average water content, the *D(θ)* is known diffusivity function. Eq. (15.19) can be integrated to obtain cumulative infiltration.

Gardner (1959) presented the analytical solution for the second stage of evaporation by using the solution for diffusion by Crank (1956). According to Crank (1956), the weighted mean diffusivity for desorption $(\bar{D}(\theta))$ is

$$\bar{D}(\theta)=\frac{1.85}{(\theta_i-\theta_0)^{1.85}}\int_{\theta_0}^{\theta_i} D(\theta)(\theta_i-\theta)^{0.85}\mathrm{d}\theta \tag{15.20}$$

$\bar{D}(\theta)$where for sorption process is higher than that for desorption process. The weighing is done differently because in infiltration maximal flux occurs at the wet end of column, where diffusivity is the highest. However, in drying the greatest flux is through the dry end, where diffusivity is the lowest. This is also the reason, why sorption processes are faster as compared to desorption. Gardner (1959) assumed that initial evaporation is infinitely high and soil surface is instantaneously brought to the final stage of drying. Therefore, $e_{\mathrm{pot}}\rightarrow\infty$, at $t=0$ when second stage of drying starts. Using the diffusivity form of Richards' equation and assuming that influence of gravity is negligible, the evaporation rate for a semi-infinite soil column can be given as

$$e=(\theta_i-\theta_0)\left(\frac{\bar{D}(\theta)}{\pi t}\right)^{1/2} \qquad (15.21)$$

and cumulative evaporation *(E)* can be given as

$$E=2(\theta_i-\theta_0)\left(\frac{\bar{D}(\theta)t}{\pi}\right)^{1/2} \qquad (15.22)$$

Using the sorptivity concept of Philip (1975), Rose (1966) presented the following relationship for evaporation calculation in the second stage of drying:

$$E=S' t^{1/2}+A't \qquad (15.23)$$

or

$$e=\frac{1}{2}S't^{-1/2}+A' \qquad (15.24)$$

where *S′* is the soil evaporativity (which is equivalent to soil water sorptivity in infiltration, since the process is drying it can be termed as desorptivity, $LT^{-1/2}$) and *A* is a constant (LT^{-1} comparable to trasmissivity [see Eq. (14.24)]). The value of *S′* is positive whereas *b* is negative. The assumption of a zero flux at the bottom of the profile or at depth *L*, although simple, implies that in the absence of this condition evaporation will accompany redistribution. This will reduce both the evaporation rates and the duration of the first stage. Solutions of evaporation considering isothermal conditions differ from the nonisothermal condition. The concept of three stages of evaporation does not strictly hold in field conditions (Jackson et al., 1973). The diurnal temperature fluctuations and other atmospheric process largely affect the evaporation rate. When air temperatures are low the upward heat flow is accompanied with water flow. When temperatures are high, the downward heat flow is accompanied with water flow and/or vapor flow. All these effects make sure that the second stage of drying starts well before the moisture content of soil has reached hygroscopic coefficient or the final dry value. Another factor, which can influence evaporation by as much as 50% is the presence of cracks in the soil. The cracks or similar soil inhomogeinities have totally different thermal fields compared to homogeneous soils. Downward vapor flow due to thermal gradients is observed within the cracks of small sizes (Hatano et al., 1988). The cracks may not increase the evaporation rate during the early stage of drying, but can increase the duration of that stage. Cracks can also increase the evaporation rate of subsequent profile controlled drying period (or second stage).

15.4.5 Nonisothermal Evaporation

The isothermal flow equation is assumed to predict the constant and falling rate of evaporation reasonably well. The role of nonisothermal conditions is explained by comparing the solutions of an isothermal process to the solutions of nonisothermal process (Milley, 1984). According to Jackson et al. (1974), in wet soils the thermal and isothermal vapor fluxes are approximately equal and opposite in direction for diurnal variation of temperature. For a dry soil surface layer, the thermal vapor pressure increases the evaporation from soil profile during night. However, neglecting thermal effects over a month introduce only about 1% error.

15.5 MANAGEMENT OF EVAPORATION

Evaporation from bare soil surface needs to be reduced so that moisture status of soil can be maintained at a stage favorable for crop growth and production. The evaporation management can be done by: (i) reducing the total amount of incident radiations or sources of energy responsible for evaporation; (ii) modifying the color of soil by applying amendments and changing the albedo parameters; and (iii) reducing the upward flux of water by either lowering the water table, or decreasing the diffusivity and conductivity of the soil profile. The methods of evaporation reduction from bare soils depend on the stage of drying. The first stage requires modifications, which will alter meteorological conditions of the surroundings. The second stage requires measures, which will change water transmission properties of the soil profile. Covering or mulching the surface with vapor barriers or with reflective materials can reduce the intensities of the incoming radiations and reduce the evaporation in the first stage of drying. A deep tillage may change the variation of diffusivity with changing water content of soil profile and may change the rate at which water can be supplied to the soil surface from underneath for evaporation.

15.5.1 Mulching

Mulch is any material placed on a soil surface primarily to cover the surface for the purpose of reducing evaporation, controlling weeds, and obtaining beneficial changes in soil environment. The other benefits of mulching are: (i) reducing soil erosion; (ii) sequestering carbon; (iii) providing organic matter and plant nutrition; (iv) regulating and moderating soil temperature; (v) increasing earthworm population and improving soil structure; and (vi) reducing soilborne diseases.

Mulches can consist of many different types of materials, such as sawdust, manure, straw, leaves, crop residue, gravels, paper, and plastic sheets, etc. (Fig. 15.7) (Lal, 1991). Paper or plastic mulches, especially light colored, are effective in reducing the effects of meteorological variables, which influence the evaporative demand during the first stage of soil evaporation (Figs. 15.8 and 15.9). Black paper and plastic mulches are effective in weed control (Fig. 15.10). The temperature of the soil under plastic mulch can be 8 to 10°C higher than under straw mulch. Soil thermal regime is a function of the contact coefficient, which is a product of thermal conductivity and volumetric heat capacity of the soil (refer to Chapter 17). A mulched plot with dry crop residue is equivalent to a two-layered profile of which the upper layer has a lower contact coefficient. Therefore, temperature variations in the soil underlying the mulched layer are reduced (Figs. 15.11 and 15.12). High temperature may be beneficial to the crops on temperate regions during germination in spring. However, high temperature during summer and in the tropics may adversely affect the growth of temperature-sensitive crops. Other mulch materials may include preparations of latex, asphalt, oil, fatty acids, and alcohols. These materials can be used as mulches for reducing evaporation from soil surface. Hillel (1976) proposed that uppermost layer of soil be formed by clods or a rough seedbed, which are treated with water proofing materials (e.g., silicones). These waterproof clods act as dry mulch and reduce evaporation and erosion from soil surface.

Vegetative mulch must have sufficient thickness to be effective in reducing evaporation and risks of soil erosion. The porosity and hydraulic conductivity of the vegetative mulches are high, and therefore diffusion or

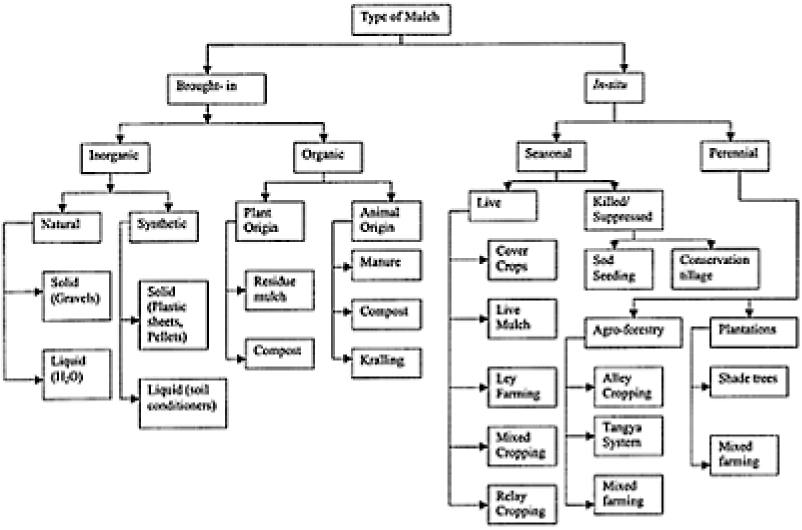

FIGURE 15.7 Type of mulches on the basis of the source of the material. (Modified from Lal, 1991.)

FIGURE 15.8 Clear plastic mulch used on cassava grown at IITA in western Nigeria to conserve soil water.

FIGURE 15.9 Clear plastic mulch used on a ridged seed bed. Note holes in the plastic for seedling emergence.

FIGURE 15.10 Black plastic mulch to conserve water and control weeds in strawberries grown in California.

airflow through the vegetative mulch is also high. A mulch of small thickness may be mostly ineffective. Vegetative mulches are light colored and reflect most of the incident radiations. Therefore, the initial evaporation rate under mulch is generally less. Gravel mulching is a common practice of water conservation, as it enhances the infiltration and simultaneously suppresses evaporation and reduces erosion of soil. Disadvantages of gravel mulch are that gravel cannot be removed from the field after application and can adversely affect future land uses.

15.5.2 Tillage

Among the various soil management practices for weed control and seedbed preparation, tillage is an important technique of soil manipulation. Tillage operations generally result in opening up of soil, changes in structure, loosening of tilled soil, and compaction of soil immediately below the tilled layer (Fig. 15.13) (Lal 1989, 1990). The opening of the topsoil enhances the evaporation from the tilled soil layer. However, the compaction of layers underneath might reduce the upward transmission of water and subsequently make the water availability limiting and reduce evaporation. The reduction of diffusivity in the soil layer also reduces the evaporation. The discontinuity of pore channels due to the

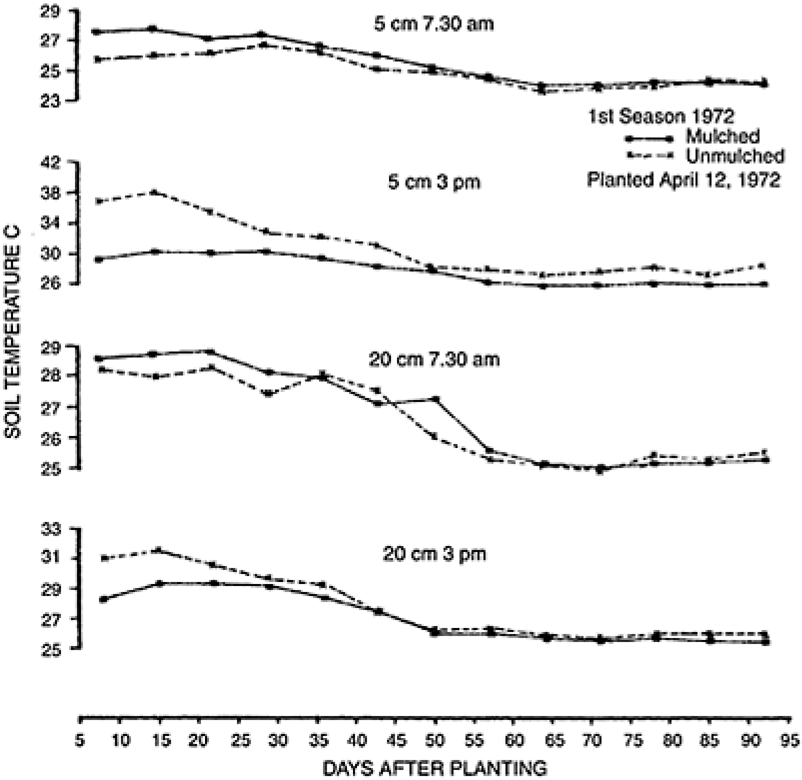

FIGURE 15.11 Effects of mulching on soil temperature under maize. (From Lal, 1974.)

tillage operations does not reduce the upward flow of water and does not reduce the total evaporation. More recent trends have indicated that management practices involving minimum tillage are better for efficient soil management. The tillage is beneficial under two situations: (i) in soils with high swell-shrink capacity and where frequent wetting and drying produces cracks. These cracks are the sources of secondary evaporation from soil. Cultivation may prevent development of or help obliterate cracks, (ii) Tillage eliminates weeds and may reduce the rate of application of herbicides. Burning crop residue and the presence of ash on the soil surface can influence soil temperature by altering albedo and soil moisture regime (Figs. 15.14 and 15.15).

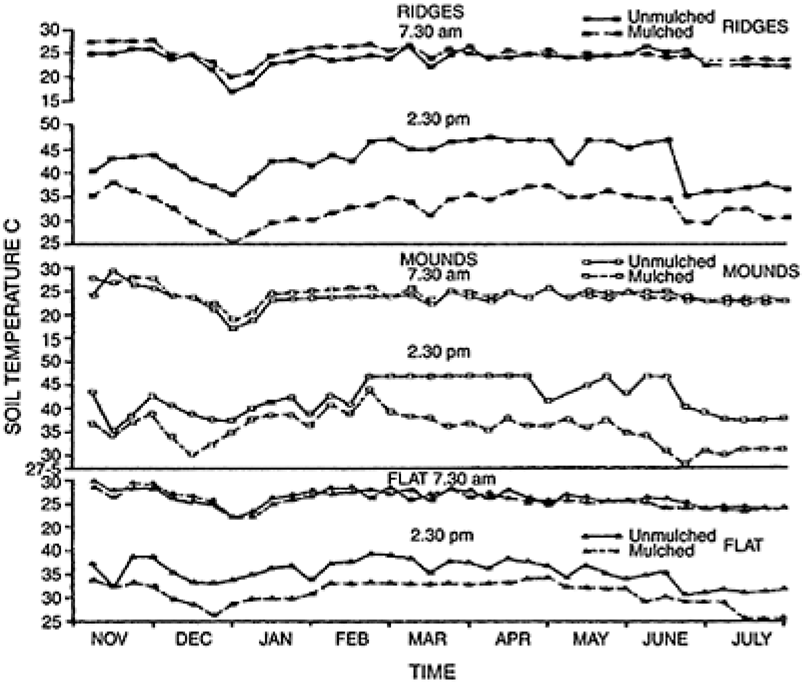

FIGURE 15.12 Effect of mulching and methods of seedbed preparation on soil temperature under yams. (From Lal, 1974.)

15.5.3 Conservation Tillage

Conservation tillage practices leave a high percentage of the residues from previous crops on the soil surface (Fig. 15.16). Plant residues left on the soil surface are effective in reducing evaporation and conserving soil moisture. A conservation tillage practice widely used in semiarid and humid regions is stubble mulching where wheat stubbles or corn stalks from previous crops are uniformly spread over the soil surface. The land is then tilled with special implements, which leave most of the residue on the soil surface. The next crop is planted through the stubble, which results in a healthy environment (temperature, water, and air) for seed germination. No tillage, or zero tillage, is another conservation tillage system that leaves residue on the soil surface and a new crop is planted directly through the residue of the previous crop with no plowing or disking (Lal, 2003).

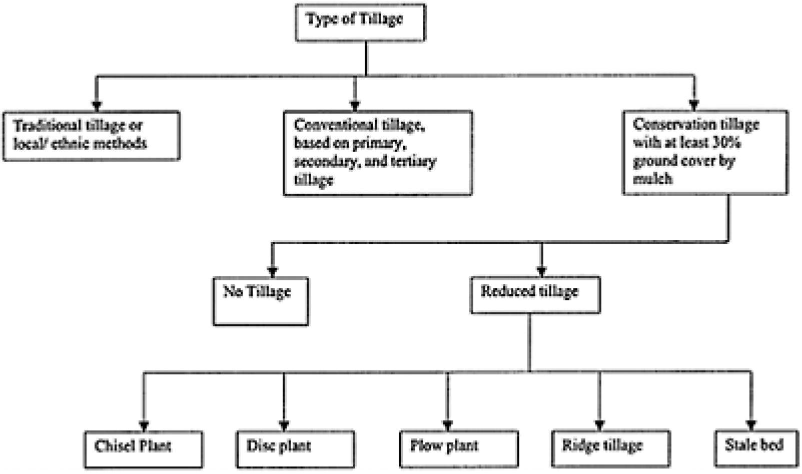

FIGURE 15.13 Types of tillage methods. (Modified from Lal, 1989; 1990.)

FIGURE 15.14 Burning crop residues in a mounded seed bed in Ethiopia. Mounded seedbed alters soil temperature and affects evaporation rate.

FIGURE 15.15 A mulch cap on yam mounds decreases soil temperature and reduces evaporation (right), while ash from crop residue alters albedo and soil temperature.

FIGURE 15.16 No-till farming with crop residue mulch reduces soil evaporation.

Example 15.1

Assume average daily steady state evaporation is 1 cm in a saturated loam soil in a high water table area. Estimate (a) threshold depth beyond which water table must be lowered, (b) water table depth at which evaporation will fall to 20% of potential value, and (c) plot daily evaporation rate with respect to water table depth. Use Eq. (15.10), assuming Aa to be equal to 4.5 cm^2.sec and n=3.

Solution

According to Eq. (15.10)

$$q_{\max} = \left(\frac{Aa}{d^n}\right) \Leftrightarrow d = \left(\frac{4.5}{1/86400}\right)^{1/3} = 72.99 = 73\,\text{cm}$$

where d is the maximum depth of water table below the soil surface, which can supply water to maintain a steady flux for evaporation. Hence

(a) Threshold water table depth is 73 cm.

(b) The water table depth ($d_{0.2}$) at which evaporation rate falls by 20% can be calculated from again Eq. (15.10) as follows:

$$d_{0.2} = \left(\frac{4.5}{1 * 0.2/86400}\right)^{1/3} = 124.8 = 125\,\text{cm}$$

(c)

D (cm)	$q_{\max}$ (cm)
0–73	1
80	$4.5/80^3$=0.76
90	$4.5/90^3$=0.53
100	0.39
120	0.23

Example 15.2

Consider an infinite sandy loam soil profile, which is initially saturated with water. The initial moisture content of soil is 0.52 cm3 cm^{-3} and final moisture content of 0.2 cm^3 cm^{-3}. If weighted mean diffusivity of soil is 80 cm^2 d^{-1}, calculate evaporation and the evaporation rate for each day during the next 10 days.

Solution

From Eq. (15.21) the evaporation rate *(e)*, and from Eq. (15.22), the cumulative evaporation (E), can be calculated for days 1, 2, 3... 10 as follows:

Mid-day	e (cm d^{-1})	Day	E (cm)
0.5	2.28	1	3.23
1.5	1.32	2	4.57
2.5	1.02	3	5.59
3.5	0.86	4	6.46
4.5	0.76	5	7.22
5.5	0.69	6	7.91
6.5	0.63	7	8.54
7.5	0.59	8	9.13
8.5	0.55	9	9.69
9.5	0.52	10	10.21

PROBLEMS

1. If the composite coefficient Aa is 4.5 cm^2 /s, n=3, potential rate of evaporation is 8 mm/d to what depth must the water table be lowered for reducing evaporation? Also calculate the watertable depth at which the evaporation rate drops by 10%, 30%, and 70% of potential evaporation rate.

2. Assume an infinitely deep, saturated sandy loam soil profile under very high evaporativity. If initial volumetric water content of soil is 0.50, final volumetric water content is 0.10 and weighted mean diffusivity is $2\times10^4 mm^2 d^{-1}$. Calculate the evaporation and evaporation rate, for the next 6 days.

3. If an impermeable layer exists at the end of a uniform wetted soil of depth 1.2 m, initial volumetric water content (θ_o) 0.24, and initial diffusivity $(D(\theta_o))$ $4\times10^4 mm^2 d^{-1}$. If evaporativity is 10 mm/d, calculate evaporation rate during the first 10 days if diffusivity $(D(\theta))$ is given by Eq. (15.17) are assuming B=15, calculate $D(\theta_o)$ for the next 6 days.

4. Briefly outline techniques of regulating soil evaporation and explain the principle of their effectiveness in reducing evaporation.

5. What should be the irrigation strategy in arid environments and why?

REFERENCES

Hatano R., H. Nakamoto, T.Sakuma, and H.Okajima (1988). Evapotranspiration in cracked clay field soil. Soil Sci. Plant Nutr. 34:547–555.

Gardner W.R. (1958). Some steady state solutions of the unsaturated moisture flow equation with application to evaporation from a watertable. Soil Sci. 85(4): 228–232.

Crank J. (1956). The mathematics of diffusion. Oxford University Press, London and New York.

Fisher R.A. (1923). Some factors effecting the evaporation of water from soil. J. Agr. Sci. 13:121–143.

Gardner W.R. (1959). Solutions of the flow equation for the drying of the soils and other porous media. Soil Sci. Soc. Am. Proc. 23:183–187.

Gardner W.R. and D. Hillel (1962). The relation of external evaporative conditions to the drying of soils. J. Geophys. Res. 67:4319–4325.

Gardner W.R. and M.S.Mayhugh (1958). Solutions and tests of the diffusion equation for the movement of water in soil. Soil Sci. Soc. Am. Proc. 22:197–201.

Hillel D. (1976). On the role of soil moisture hysteresis in the suppression of evaporation from bare soil. Soil Sci. 122:309–314.

Hillel D. (1980). Fundamentals of soil physics. Academic Press, New York.

Hillel D. and C.H.M.van Bavel (1976). Dependence of profile water storage on soil hydraulic properties: a simulation model. Soil Sci. Soc. Am. J. 40:807–815.

Jackson R.D., B.A.Kimball, R.J.Reginato, and S.F.Nakayama (1973). Diurnal soil water evaporation: comparison of measured and calculated soil water fluxes. Soil Sci. Soc. Am. Proc. 38:861–866.

Lal R. (1974). Role of Mulching Techniques in Tropical Soil and water management. Tech. Bulletin no. 1, International Institute of Tropical Agriculture, Nigeria.

Lal R. (1989). Conservation tillage for sustainable agriculture. Adv. Agron. 42: 85–197.

Lal R. (1990). Soil erosion in the tropics: Principle and Management. McGraw Hill Book Co., 579 pp.

Lal R. (1991). Soil Structure and sustainability. Journal of sustainable Agriculture. 1(4): 67–92.

Lal R. (2003). Historical development of no-till farming. In R. Lal, P. Hobbs, N. Upof[1], and D.O. Hansen (eds) Sustainable agriculture and the rice wheat system. Marcel Dekker, New York.

Milley P.C.D. (1984). A linear analysis of thermal effects on evaporation from soil. Water Resour. Res. 20:1075–1086.

Moore R.E. (1939). Water conduction from shallow watertable. Hilgardia 12: 383–426.

Pearse J.F., T.R. Oliver, D.M. Newitt (1949). The mechanisms of the drying of solids: Part I. The forces giving rise to movement of water in granular beds during drying. Trans. Inst. Chem. Eng. (London) 27:1–8.

Philip J.R. (1957). Evaporation, moisture and heat fields in soil. J. Meteorol. 14: 354–366.

Ripple C.D., J. Rubin, and T.E.A. van Hylckama (1972). Estimating steady state evaporation rates from bare soils under conditions of high water table. US Geol. Surv. Water-Supply Paper 2019-A.

Rose C.W. (1966). Agriculture Physics. Pergamon Oxford.

Willis O.W. (1960). Evaporation from layered soils in presence of a watertable. Soil Sci. Soc. Am. Proc. 24:239–242.

16
Solute Transport

16.1 INTRODUCTION

Water entering the soil profile from rain or irrigation is essentially a dilute solution. Rainwater is pure when it condenses to form clouds; during descent it absorbs atmospheric gases (i.e., CO_2, N_2, products of sulfur and O_2, etc.). When water flows on soil surface as overland flow and/or through the soil matrix, it also dissolves solutes (e.g., salts, fertilizers, pesticides). These solutes not only move with soil water but also within the soil matrix mainly due to the concentration gradients. Sometimes, solutes react among themselves and/or with soil material according to a range of physical and chemical processes.

In agricultural ecosystems, solutes may be categorized on the basis of their function (e.g., nutrients, pesticides, waste compounds, salts, organic chemicals, heavy metals, viruses, and bacteria). Understanding transport of solutes in soil is important to many management problems in agriculture. It can help when developing procedures for maximizing the effective use of fertilizers or pesticides and other chemicals within the root zone while minimizing their movement into groundwater. Knowledge of these processes is important to understanding the problems of contamination of natural water through leaching or redistribution within a vadose zone to groundwater, availability of solutes for plant uptake, surface runoff, salt intrusion in coastal aquifers, seepage from storage or disposal systems, and chemical residues.

Depending upon chemical stability and reactivity, the solutes are broadly classified into two categories: (i) conservative solutes, which remain unchanged physically and chemically, and do not undergo irreversible reactions, such as chloride (Cl) and bromide (Br); and (ii) nonconservative solutes, which can undergo irreversible reactions and change their physical or chemical phase. The nonconservative solutes can be divided into labile solutes and reactive solutes. The labile solutes can undergo reversible or irreversible physiochemical, biochemical, or microbial reactions and can change their physical or chemical phase with time. The examples of labile solutes are: nitrate, sulfate, and ammonia, which are involved in mineralization, immobilization, or redox reactions. Some pesticides are also labile and their lability is quantified by their half-life (White et al., 1998). Reactive solutes undergo reversible or irreversible reactions with soil constituents by way of adsorption (adsorption of cations, e.g., Ca^{+}, Mg^{++}, on clay particles), precipitation or dissolution (e.g., precipitation of calcium as calcium sulfate or calcium carbonate). The anions (e.g., such as nitrate (NO_3^-), Cl^-, and Br^-), which are weakly adsorbed on positively charged sites, are known as nonreactive solutes. The transport of reactive and nonreactive solutes through soil is affected relative to the movement of water (Nielsen et al., 1986).

Some solutes are already present in the water-filled pore space of the soil. These solutes may be present in the soil owing to: (i) mineralization of organic matter, (ii) saline groundwater intrusion, (iii) fertilizer and/or pesticide application, (iv) atmospheric deposition, and (v) weathering of mineral. When solute-free water flows through the soil matrix, the concentration of these preexisting solutes is the highest in those pores experiencing the lowest water flux. Apart from the preexisting, solutes are also applied on soil surface (e.g., fertilizer, pesticides, etc.). Basically solute transport within a soil matrix occurs by two physical processes: diffusion and convective flow. Several simple and complicated mathematical models have been developed in the past, which can reproduce the experimental results very well. Most of these models are developed for the macroscopic scale (Nielsen et al., 1986), although pore scale description is available (e.g., Navier–Stokes equation). This chapter describes the transport mechanisms in more detail and discusses the transport models on a macroscopic scale.

16.2 SOLUTE TRANSPORT PROCESS

The movement of solutes inside the soil matrix is caused by “mass flow” or “convection.” This type of flow is also called *Darcian flow* (see Chapter 12). The velocity at which solutes travel through soil matrix is generally known as “pore water velocity” and is the ratio of volumetric flow of solute through a unit cross-sectional area and volumetric moisture content of the soil matrix. In other words, the pore water velocity is the ratio of Darcian velocity and moisture content. In general, pore water velocity accounts for the straight-line length of path traversed in the soil in a given time. In reality, the flow paths are not always straight but are irregular or tortuous. This property is known as “tortuosity” of soil pores. Solutes do not always flow with water but sometimes go ahead of it due to the twin process of diffusion and dispersion or exclusion, lag behind due to adsorption or retardation, or get precipitated or volatilized. The movement of solute from the higher concentration to the lower concentration gradient is also known as the process of “diffusion.” This process commonly occurs within gaseous and liquid phases in the soil matrix due to the random thermal motion, also called “Brownian movement.” There is another simultaneous process that tries to mix and eventually even out the concentration gradients known as “hydrodynamic dispersion.” Diffusion is an active process, whereas dispersion is a passive process. However, in most practical applications these two solute transport processes are considered additive.

Some chemicals, which are soluble in water and have a nonnegligible vapor phase, can exist in three different phases in a soil matrix: as a dissolved solute in soil water, as a gas in soil air, and as an ion absorbed on the soil organic matter or charged clay mineral surfaces. Therefore, all solute concentration terms are not equal in dimensions and depend on the concentration in these soil phases and the partitioning of these phases. The total solute resident concentration (C, g cm^{-3}) in a soil matrix can be mathematically expressed as

$$C={}_{\rho b}C_a+\theta C_1+f_aCg \tag{16.1}$$

where ρ_b is the soil bulk density (gcm^{-3}), C_a is adsorbed concentration (g g^{-1}), θ is volumetric soil moisture content (cm^{3}cm^{-3}), C_1 is dissolved solute concentration (gcm^{-3}), fa is the volumetric air content (cm^3 cm^{-3}), and C_g is gaseous solute concentration (gcm^{-3}). Soil physical parameters (ρ_b, θ and f_a) weight the solute concentrations in the three phases of soil on a volume basis, and convert different reference dimensions to cm^3 of soil. The resident concentration is the volume-averaged concentration in soil, which is measured by extracting a known volume of soil in water. The resident concentration is expressed as the mass of solute per unit volume of soil water to make it comparable to flux-averaged concentration. The flux concentration is the solute concentration in water flowing through the soil.

16.3 MACROSCOPIC MIXING

Several different mechanisms operating in the porous media during transport of solute are responsible for the mixing at macroscopic level. Some of these include the following (Greenkorn, 1983):

1. *Molecular diffusion:* If the process is stationary or slow moving and the time required for the solute to move through the porous media is sufficiently long (i.e., for sufficiently long time scale) molecular diffusion is the primary source of macroscopic mixing.
2. *Tortuosity.* The tourtuous flow paths inside the soil profile causes the fluid element to remain at different distances from the same starting position even when they travel at the same pore water velocity (ratio of Darcy velocity and soil moisture content).
3. *Connectivity of pores:* If the pores are not well interconnected or if some of the pores in the porous media are not accessible to the fluid element flowing through that pore, they cause macroscopic mixing and dispersion.
4. *Hydrodynamic dispersion:* The solute element near the wall of pore travels at a different velocity than the element at the center of pore (Fig. 16.1a). This results in a velocity gradient inside the pore and solute elements move relative to each other at different velocity.
5. *Immobile zones:* The immobile water zones normally causes the fluid element to move quicker and out in the effluent solution earlier (early breakthrough), and at the same time, increases the tail of the breakthrough curve mainly due to the slow release of solute element trapped inside immobile water (see Sec. 16.12).
6. *Turbulence:* If the size of the pore abruptly changes, the flow inside a pore may become turbulent and mixing is caused by eddies.
7. *Adsorption:* When the concentration front looses some ions abruptly as they are removed from solution by the process known as adsorption, the unsteady state flow occurs and the concentration profiles becomes flat.

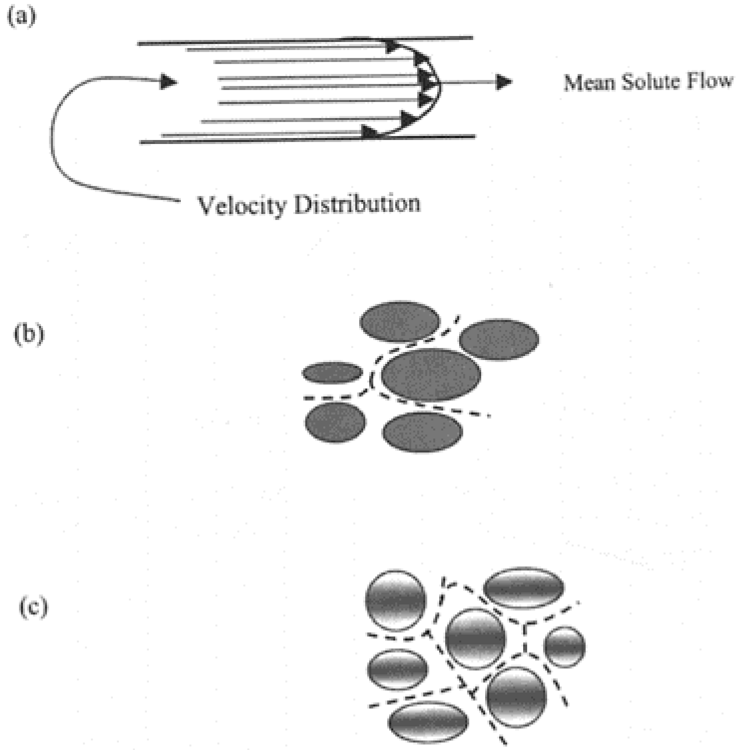

FIGURE 16.1 The physical mechanisms for hydrodynamic dispersion of solutes through soil matrix: (a) influence of velocity distribution within a soil pore; (b) influence of size of pore, and (c) influence of microscopic flow direction.

16.4 FICK’S LAW

There are two Fick’s laws, which describe diffusion of substances in porous media. The movement of ions from areas of higher concentration to lower concentration is proportional to the concentration gradient, the cross-sectional area available for diffusion, and the elapsed time during the solute transport. The net amount of solute crossing a plane of unit area in unit time is known as the solute flux density (J; $gcm^{-2}s^{-1}$), which is given by Eq. (16.2) known as Fick’s first law (1855) for steady state one-dimensional solute transport:

$$J = -D_m \frac{\partial C}{\partial x} \qquad (16.2)$$

where D_m is the ionic or molecular diffusion coefficient of the porous media ($cm^2 s^{-1}$), C is the solute concentration (gcm^{-3}) and x is the distance (cm). The concentration gradient $(\partial C/\partial x)$ in Eq. (16.2) is the driving force and the minus sign indicates that solute moves from areas of higher concentration to lower concentration. The molecular diffusion coefficient in Eq. (16.2) varies with soil physical and chemical properties of soil and solute (i.e., soil texture, soil moisture content, solute cocentration, and pH), soil solute interactions, and temperature. The solute concentration follows a normal, or Gaussian, distribution and can be described by the mean and variance. The depth of penetration (X_p) of a diffusing ion in soil for a given time duration (t) can be estimated by the root mean-square displacement as follows:

$$X_p=(2D_m t)^{1/2} \qquad (16.3)$$

Diffusion in soils is a relatively slow process and operates over small distances, thus maintaining the electrical neutrality of ions. For transient state condition, Eq. (16.2) is coupled with the one-dimensional mass conservation equation with no production or decay taking place during solute transport through soil

$$\frac{\partial C}{\partial t} = -\frac{\partial J}{\partial x} \qquad (16.4)$$

Equation (16.4) implies that the net change in solute concentration is as a result of net change in rate of flow. Combining Eqs. (16.2) and (16.4) and assuming that D_m is independent of solute concentration and depth, results in Fick's second law for one-dimensional transient solute flow

$$\frac{\partial C}{\partial t} = D_m \frac{\partial C^2}{\partial x^2} \qquad (16.5)$$

16.5 TRANSPORT EQUATIONS

When a solute enters a soil matrix (which can be in a soil core, repacked soil column, or agricultural soil in a field) the initial sharp boundary between the resident and displacing solute starts diminishing mainly due to the twin processes of diffusion and dispersion. The transport of a solution through soil matrix consists of three main components: convection, diffusion, and dispersion, which are briefly described below.

16.5.1 Convection or Mass Transport

Convective or advective transport of a solution inside a soil matrix is known as the passive movement with flowing soil water. If the transport process has only convective transport without any diffusion, the water and solute move at the same average flow rate. Mathematically convective transport (J_m) can be expressed as

$$J_m = q_s C \tag{16.6}$$

where J_m is the flux density for convective or mass transport ($ML^{-2}T^{-1}$), q_s is the volumetric fluid flux density with dimensions of velocity (LT^{-1}), and C is the volume averaged solute concentration (ML^{-3}). The flux density of water can be calculated by the Darcy equation for a steady state flow of water. The q_s is also analogous to θ, where v is the pore water velocity (LT^{-1}).

16.5.2 Diffusive Transport

Diffusion is a spontaneous process resulting from the random thermal motion of dissolved ions and molecules. In general, the diffusion is an active process and diffusive transport tends to decrease the existing concentration gradients and moves the process towards homogeneity rather rapidly. Fick's law defines the diffusive transport and for one-dimensional steady state transport is given as:

$$J_D = -D_m \frac{\partial C}{\partial x} \tag{16.7}$$

where J_D is solute flux density for diffusive transport of solute ($ML^{-2}T^{-1}$), θ is the volumetric moisture content (L^3L^{-3}). The diffusion coefficient in soils (D_m) is slightly less than the diffusion coefficient in pure water (D_0) mainly due to the tortuous flow paths in soils.

$$D_m = D_0 \theta \xi \tag{16.8}$$

where ξ is the dimensionless tortuosity factor ranging roughly from 0.3 to 0.7 for most soils.

16.5.3 Dispersive Transport

The soil matrix consists of pores of different shapes, sizes, and orientation. This heterogeneity of pore structure causes a large deviation of local pore water velocities inside each individual pore. Consider a one-dimensional flow through a single capillary tube of constant radius R. According to Poiseuille's law, the flow rate through each pore varies proportional to the fourth power of the radius R (Kutilek and Nielsen, 1994). However, the flow velocity (v) through the tube is a decreasing function of radial distance (r) from the center of tube. If average velocity is v' then $v=2v'(1-(r^2/R^2))$, when $r=R$, i.e., at the wall of pore v $=0$, and at $r=0$, i.e., at the center of pore $v=2v'$. It is, therefore, clear that microscopic scale variations of pore water velocity in the soil matrix are very important and large.

Dispersive transport occurs because of the velocity variations in soil matrix with respect to average pore water velocity. The velocity variations in a soil matrix is caused by several factors such as zero velocity at the particle surface, which increases gradually and is the maximum at the center of pore or at air water interface under unsaturated conditions (Fig. 16.1a). Pore sizes also create velocity gradients with the velocity in larger pores greater than the velocity in smaller pores (Fig. 16.1b). The other possible reason is the fluctuation of flow paths of an element of water with respect to the mean direction of flow (Fig. 16.1c). Macroscopically, dispersion process is similar to the diffusion process, however, unlike diffusion, it occurs only during water movement. Field and laboratory experiments have shown that the dispersive transport can be described by an equation similar to diffusion as follows:

$$J_h = -\theta D_h \frac{\partial C}{\partial x} \tag{16.9}$$

where D_h is the mechanical dispersion coefficient (Bear, 1972) and is assumed to be a function of fluid velocity as follows:

$$D_h=\lambda v^n \tag{16.10}$$

where λ is the dispersivity and exponent "n" is an empirical constant generally assumed equal to 1.

The mixing or dispersion that occurs along the direction of flow path is called longitudinal dispersion and that in the direction normal to flow is known as transverse dispersion. Diffusion is an active process whereas dispersion is passive, in spite of this, most analysis on solute transport considers both processes to be additive because macroscopically both processes are similar.

$$D=D_m+D_h \tag{16.11}$$

where D is the longitudinal hydrodynamic dispersion coefficient (Bear, 1972) or apparent dispersion coefficient (Nielsen et al., 1972).

Combining Eqs. (16.6), (16.7), (16.9), and (16.11) leads to the following expression for solute flux, J_s

$$J_s = -\theta D \frac{\partial C}{\partial x} + qC \tag{16.12}$$

The equation of continuity states that:

$$\frac{\partial J_s}{\partial x} = -\frac{\partial}{\partial t}(\theta C + \rho_b S_s) \tag{16.13}$$

where S_s is adsorbed concentration (MM^{-1}), ρb is the bulk density (ML^{-3}), and t is time *(T)*. Combining Eqs. (16.12) and (16.13) gives the following solute transport equation

$$\frac{\partial}{\partial t}(\theta C + \rho_b S_s) = \frac{\partial}{\partial x}\left(\theta D \frac{\partial C}{\partial x} - qC\right) \tag{16.14}$$

It is well known that adsorption and exchange processes are usually nonlinear and also depend on the competing species in the soil system. Still, one of the most common approaches to describe the relationship between adsorbed and solution concentrations has been to assume instantaneous adsorption and linearity between C and S of the form (forcing the constant or intercept to zero)

$$S_s=K_D C \tag{16.15}$$

where K_D is the empirical distribution coefficient. Inserting Eq. (16.15) into Eq. (16.14) and dividing both sides with θ results in Eq. (16.16):

$$\frac{\partial}{\partial t}\left(C+\frac{\rho_b K_D C}{\theta}\right)=\frac{\partial}{\partial x}\left(D\frac{\partial C}{\partial x}-\frac{q}{\theta}C\right) \tag{16.16}$$

Assuming that the soil profile is homogeneous and moisture content and flux density are constant in time and space, Eq. (16.16) reduces to

$$R\frac{\partial C}{\partial t}=D\frac{\partial^2 C}{\partial x^2}-v\frac{\partial C}{\partial x} \tag{16.17}$$

where R is the retardation factor and is given by

$$R=1+\frac{\rho_b K_D}{\theta} \tag{16.18}$$

K_D in Eq. (16.15) can be obtained from the slope of sorbed concentration (MM^{-1}) versus solution concentration (ML^{-3}). A zero value of K_D in Eq. (16.18) reduces R to 1, which indicates no interactions between solute and soil. A negative value of K_D makes R less than one, which indicates anion exclusion or immobile water, which does not contribute to convective transport. In case of anion exclusion, $(1-R)$ is known as anion exclusion volume. A positive K_D results in $R>1$, which indicates sorption.

16.6 BREAKTHROUGH CURVES

When a fluid (or solute) is passed through a soil matrix containing another liquid in its pore space, the introduced fluid, which can also be called the displacing liquid or applied liquid, gradually displaces the preexisting liquid (displaced liquid). Analysis of the collected effluent from soil matrix at a given depth (or from one end of a repacked soil column) shows a change in composition of effluent solution with respect to time. If the displacing and displaced solutions are not mutually soluble, the process is called “immiscible” displacement (e.g., oil and water). On the other hand, if both solutions are soluble, the process is called “miscible” displacement (e.g., aqueous solutions). The graphical representation of the concentration of these solutes with respect to time or cumulative effluent volume or pore volume is known as “breakthrough curves” (BTC). Pore volume is the ratio of cumulative effluent volume (cm^3) at a specified time and total volumetric moisture content of soil (cm^3). Pore volume is a nondimensional number and is zero at time zero.

16.6.1 Solute Input

As is evident in Figs. 16.2a–c, BTCs can have different shapes depending upon the solute application. Figure 16.2a shows a BTC where effluent solute concentration increases and reaches a maximum and then remains constant thereafter. The y-axis on Fig. 16.2 is the relative solute concentration (C/C_0), which is the ratio of concentration of effluent solute collected at a given time (C) and the concentration of displacing or incoming solution (C_0). The BTC in Fig. 16.2a is for a step input of displacing solute or tracer, where applied solution displaces all the preexisting solution gradually.

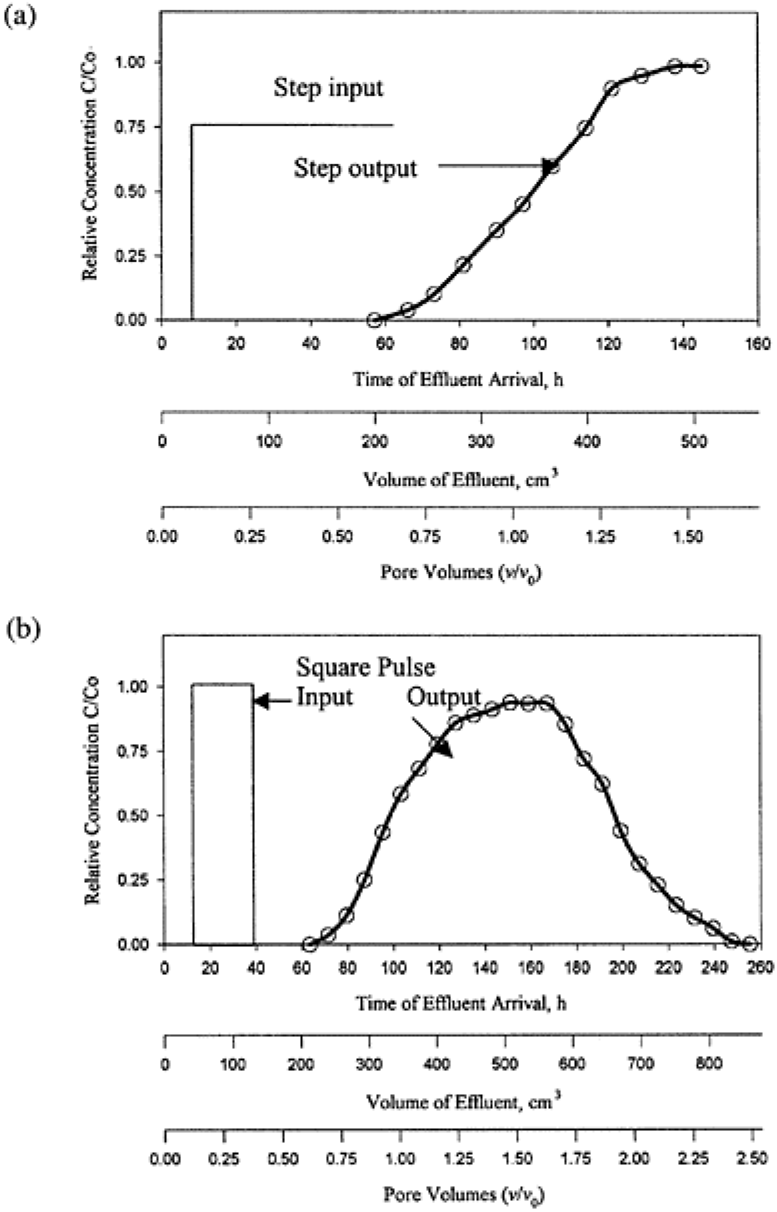

FIGURE 16.2 Breakthrough curves with respect to time of effluent arrival, volume of effluent, and pore volumes, (a) Chloride application as a step input through a 10 cm loam soil column

(pore water velocity=0.11 cm.h^{-1}); (b) chloride application as a pulse input through a 10 cm loam soil column (pore water velocity=0.1 cm.h^{-1}); and (c) schematic for a Dirac and square pulse input and output. (Modified from Shukla et al., 2002.)

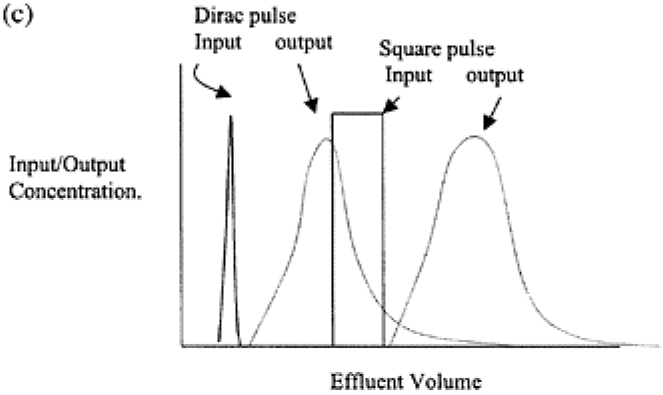

Therefore, the concentration of applied solution increases whereas that of the preexisting solution decreases with time. If the application of displacing or applied solution continues, it attains the maximum concentration equal to C_0. The ETC in Fig. 16.2b is obtained from a predetermined volume of the displacing solution followed by the original or preexisting solution. This type of solute application is known as “pulse” application. A pulse application can be: (i) a distributed pulse, (ii) a dirac pulse, and (iii) a square pulse. The concentration of solution applied as a distributed pulse gradually increases, attains a maximum, and then gradually goes down to zero (Fig. 16.2b). A solute pulse application for an infmitesimally short period is known as a “dirac pulse” (Fig. 16.2c). When time for solute pulse application is much smaller than time of leaching, it is called a dirac pulse input (e.g., single application of highly soluble fertilizer, pesticide, etc.). A square pulse is a step-up change followed by a step-down change, and the ETC shows a steep rise followed by steep fall (Fig. 16.2c).

16.6.2 Some Interpretations of Breakthrough Curves

Pore volumes are defined as the ratio of the volume of displacing water (V, water entered or flowed out at a given time), and the volumetric moisture content of the soil (V/V_0). Assuming that the moisture content of soil in a repacked column is 0.5cm^{3}cm^{-3} (or 50%) and the total volume of soil column is 100 cm^3, therefore, volumetric moisture content of the repacked soil column is 50 cm^3. Once 50 cm^3 of displacing solution is passed through the soil column, it corresponds to a pore volume of 1.

Soil–Solute Interactions

The ETC in Fig. 16.3a depicts a condition when a solute of a given concentration displaces another solute (such as water) in such a way that all the soil pores start contributing at the same time and the solute concentration jumps from zero to the maximum (C_0) as soon as 1 pore volumes of displacing solution passes through the soil column. This type of flow is known as a "piston flow," which corresponds to pure mass flow or convection. In piston flow the entire center of solute front arrives at the end of column at the same time. Piston flow occurs in the absence of diffusion or dispersion or any type of interactions between solute and soil and solute and water move at the same velocity inside soil matrix. This type of flow is rare or near impossible under natural conditions. For known moisture content of soil and column dimensions, it is possible to calculate the number of pore volumes required before piston flow begins. The time required for a displacing solute to reach the other end of a column is known as breakthrough time, residence time, or travel time (t^*), and is equal to L/v, where L is the length of soil column. For sorbing solutes the total travel time is obtained by multiplying R and L/v.

The ETC in Fig. 16.3b shows an early arrival of displacing solute in the effluent solution (less than 1 pore volume). This process takes place because of the difference in the velocity at which water and solute travel inside the soil domain. The solute travels ahead of water because of "molecular diffusion and hydrodynamic dispersion." The ETC presented in Fig. 16.3b passes through C/C_0 of 0.5 at pore volume of 1. The area A and area B of this figure are numerically equal. This ETC represents a "convective dispersion process" with no interaction between solute and soil. The ETC in Fig. 16.3c is slightly shifted or retarded towards the x-axis. This type of shift is known as "sorption." Opposite of sorption is "repulsion" or a phenomenon of "anion exclusion" when ETC moves away from x-axis (Kutilek and Nielsen, 1994) (Fig. 16.3d).

Influence of Displacement Length

With increasing displacement length, the tortuosity and pore size distributions of the soil also increases. For a given pore water velocity, the total resident time of the solute in the soil increases with increasing displacement length. Therefore, the total mixing by convection and diffusion also increases (Nielsen and Biggar, 1962). Figure 16.4 makes it abundantly clear that if a pulse of same amount is passed through soil columns of 10, 20, and 30 cm length, the progressive attenuation of the initial concentration takes

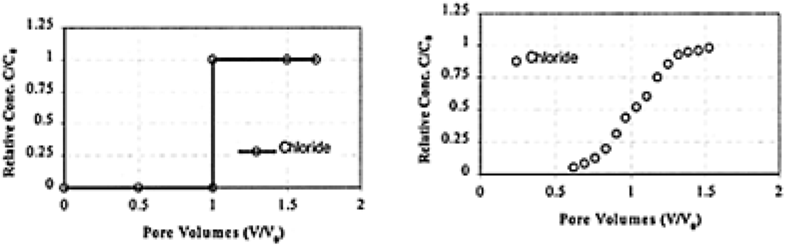

(a) Piston Flow

(b) Convective Dispersion

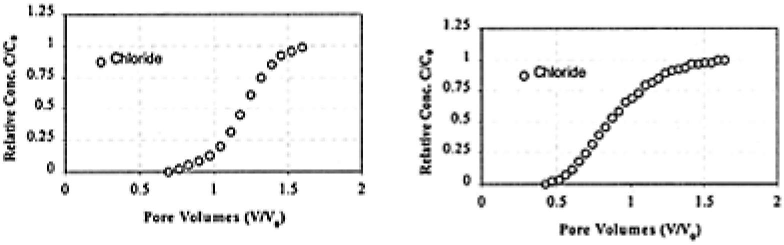

(c) Retardation/ Adsorption

(d) Anion Exclusion

FIGURE 16.3 Interpretations from experimental breakthrough curves. (Modified from Kutilek and Nielsen, 1994; Shukla et al., 2002.)

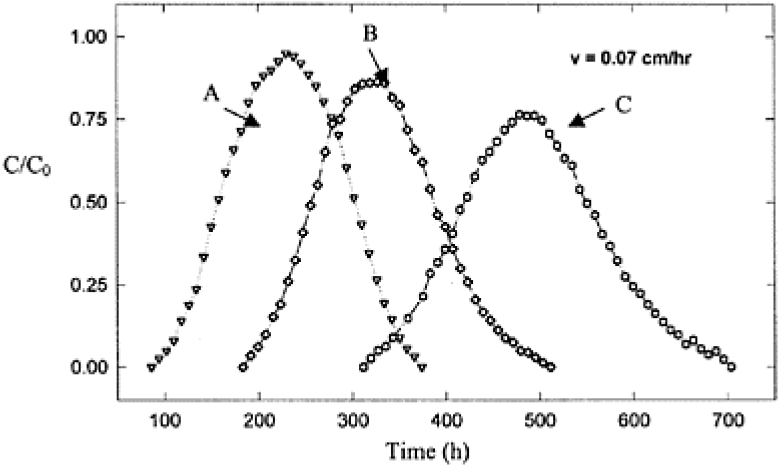

FIGURE 16.4 The progressive attenuation of BTCs for 10 cm (A), 20

cm (B), and 30 cm (C) soil columns for a pulse type chloride application through laboratory soil columns. (Redrawn from Shukla et al., 2000.)

place. This attenuation is the direct result of dilution. Therefore, solute applied as a pulse cannot carry its total mass beyond a certain depth. The total volumes of solution and total time required to completely displace the applied pulse increases with displacement length (Kutilek and Nielsen, 1994) (Fig. 16.4).

16.7 DISPERSION PROCESSES

Assuming the random capillary bundle concept (see Chapter 12), the classical dispersion theory was developed and a dispersion equation was suggested, which is similar to Fick's law and takes into account both dispersive and diffusive fluxes (Taylor, 1953; De Josselin De Jong, 1958; Bear and Bachmat, 1967; Fried and Combarnous, 1971). There are several mechanisms that cause macroscopic mixing and are generally accounted for in the dispersion coefficient. Some of them are mixing due to tortuosity, inaccessibility of pore water, recirculation due to flow restrictions, macroscopic and hydrodynamic dispersion, and turbulence in flow paths (Greenkorn, 1983). In addition, molecular diffusion, the presence of dead-end pores, sorption, exclusion, and physical nonequilibrium affect the degree of asymmetry in BTCs in different proportions (Nielsen et al., 1986).

The hydrodynamic dispersion coefficient *(D)* is proportional to the pore water velocity of a solute under steady state flow conditions (Biggar and Nielsen, 1967; Bear, 1972).

$$D \propto \frac{q}{\theta} \text{ or } v \tag{16.19}$$

$$D=\lambda v \tag{16.20}$$

The proportionality constant, A,, in Eq. (16.20) is known as dispersivity. The value of dispersivity depends upon the scale over which water flux and solute convection is averaged. Dispersivity is also dependent on the moisture content of the porous media (Krupp and Elrick, 1968) and decreases rapidly as moisture content decreases from saturation. A 10-fold increase in longitudinal dispersivity is reported when moisture content decreases from saturation (Wilson and Gelhar, 1974). Some typical values of dispersivity for laboratory soil columns range from 0.5 to 2 cm (Jury et al., 1991), 0.11 to 0.37 cm (for loam soil) and 0.14 to 0.22 cm (for sandy loam soil; Shukla et al., 2003). The dispersion processes are site specific and depend upon the subtler factors, which are related to the experimental conditions (Flury et al., 1998). The longitudinal dispersivity values are measured in field soils by placing a suction cup at different depths and measuring solute breakthough as a function of time. The dispersivity calculated for field soils by one-dimensional convective dispersion Eq. (16.23) or method of moments (Jury and Roth, 1990) are given in Table 16.1.

TABLE 16.1 Dispersivity Values Measured in Field Soils Using Suction Cups

Soil	Tracer	Application rate, cmd^{-1}	Dispersivity cm	Reference
Clay, silty clay	Cl, Tritium	2	9.4	Van de Pol et al. (1977)
Clay loam	Cl, NO_3	–	8.3	Biggar and Nielsen (1976)
Clay loam	Br	96	5.2–23	Fleming and Butters (1995)
Clay loam	Br	30, 33, 41, 67	16–38	Jaynes (1991)
Loam	Cl	9.6–19.2	29	Roth et al. (1991)
Loamy sand	Br	1.1	3.2–15.8	Butters et al. (1989)
Loamy sand	Cl, NO_3, BO_3	1.3	1–2	Ellsworth et al. (1996)
Sand	Cl	84	0.7–1.6	Hamlen and
		132	0.8–2	Kachanowski (1992)
Sand	Cl	84, 117	17, 2.7	Van Wesenbeck and Kachanowski (1991)

Source: Modified from Flury et al., 1998.

16.8 RELATIONS BETWEEN DISPERSION COEFFICIENT AND PORE WATER VELOCITY

The effective dispersion coefficient generally varies with mean microscopic flow velocity. Based upon the magnitude of the Peclet number (P, defined as vL/D, where L is a characteristic length), within the range of average pore water velocities, molecular diffusion dominates the dispersion of the solute at smaller displacement velocities and gives way to convective dispersion at greater velocities. Hence, for relatively small average pore water velocities we expect the apparent diffusion coefficient to have values close to that of the diffusion coefficient (D_o) in the soil solution, and to be only somewhat dependent on pore water velocity. At relatively large velocities, the dispersion coefficient is strongly related to pore water velocity.

The five dispersion regimes can be identified in Fig. 16.5 as (i) pure molecular diffusion; (ii) molecular diffusion and kinematic dispersion; (iii) predominant kinematic dispersion and (iv) and (v) as pure kinematic dispersion regimes (Shukla et al., 2002). In regimes ii-v, an increase in average pore water velocity increases mixing and reduces the impact of molecular diffusion in the direction of flow. Using mixing cell approximations, it can be shown that in the region $0.01<P<50$, dispersion is directly proportional to pore water velocity (Perkins and Johnston, 1963). Further

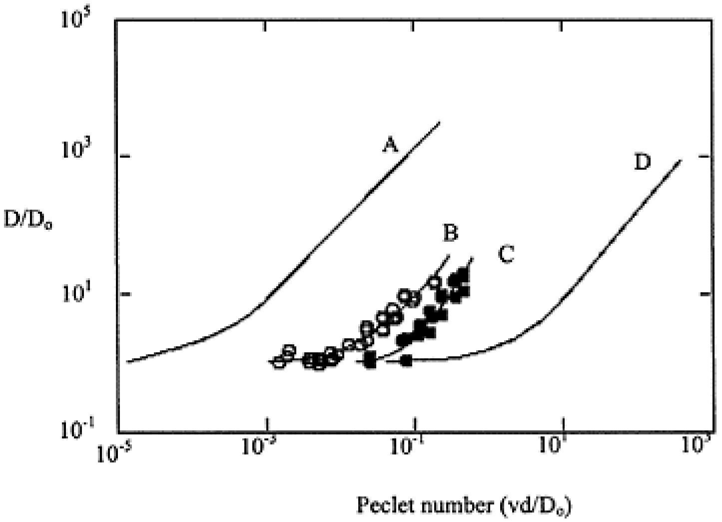

FIGURE 16.5 The relationship between DD_0^{-1} and Peclet number for: (A) field soil (A) (from Biggar and Nielsen, 1976), (B) loam, (C) sandy loam (from Shukla et al., 2002), and (D) single grain material (from Pfannkuch, 1963). (Redrawn from Shukla et al., 2002.)

increases in *P* results in a nonlinear relation to velocity ($P \propto v^n$, with $n>1$). Pfannkuch (1962) and Torelli and Scheidegger (1972) reported an n value of 1.2, Taylor (1953) of 2, Biggar and Nielsen (1976) of 1.11, and Shukla et al. (2002) of 1.71 for sandy loam and 1.21 for loam.

The relations between D/D_o and Peclet number (vd/D_o) given as solid lines in Fig. 16.5 for natural undisturbed field soil by Biggar and Nielsen (1976), and for laboratory columns of loam and sandy loam soils (Shukla et al., 2002) and for graded sands and other single-grained materials (Pfannkuch, 1962) satisfy Eq. (16.21)

$$\frac{D}{D_o} = 1 + m\left(\frac{vd}{D_o}\right)^n \qquad (16.21)$$

where

$$D_o = 0.66\theta\, D_m \qquad (16.22)$$

with D_m being the diffusion coefficient for free solution. The D_0 in Eq. (16.22) can be obtained from known values of θ and D_m (see also Chapter 18). For loam and the sandy loam soils D_0 is 0.0222 and 0.0216 cm^2 h^{-1}, respectively (Shukla et al., 2002). Other reported values of D_0 in literature are: 0.02 cm2 h^{-1} by Jury et al. (1991), 0.01 cm2 h^{-1} by Sposito (1989), and 0.0203 cm^2 h^{-1} by Shukla et al. (2003). The values of *m* increase with decreasing values of average particle diameter *d* while values of *n* range between 1 and 2 (Table 16.2). In the loam and sandy loam soils as well as the field soil, decreasing average particle diameter (increasing clay content) is associated with soil structure. The loam has relatively large pores as a result of microaggregates, and the sandy loam, although containing less clay than the loam, nevertheless has large pores also associated with its microaggregates as well as those associated with its high sand content. The field soil manifests the greatest value of *m* because of its large pore size distribution owing to its high clay content, its aggregation and its natural field structure.

16.9 MATHEMATICAL REPRESENTATION OF THE SOLUTE TRANSPORT PROCESS

The simplest form of one dimensional convective-dispersive equation (CDE), assuming macroscopic steady state water flow, constant soil– moisture content, and no interactions between the chemical and the solid phase was developed by Lapidus and Amundson, (1952), which is similar to Eq. (16.17), for R=1

TABLE 16.2 Parameters for Eq. (21) for the Results Illustrated in Fig. 16.5

Soil	m	n	d mm	D_o cm^{2}h^{-1}
Laboratory columns (mostly sand) (Pfannkuch 1962)	0.5	1.2	0.156	0.022
Sandy loam (Shukla et al. 2001)	70.5	1.71	0.0508	0.0216
Loam (Shukla et al. 2001)	141	1.21	0.0158	0.0222
Field soil (more clay) (Biggar and Nielsen 1976)	17780	1.11	0.00272	0.0250

$$\frac{\partial C}{\partial t} = D\frac{\partial^2 C}{\partial x^2} - v\frac{\partial C}{\partial x} \tag{16.22}$$

One additional term is added to Eq. (16.23) when chemical adsorption is included. Following is the one-dimensional solute transport equation describing transport through a homogeneous medium during steady state flow with adsorption [same as Eq. (16.17)]

$$\frac{\partial C}{\partial t} + \frac{\rho_b}{\theta}\frac{\partial S_s}{\partial t} = D\frac{\partial^2 C}{\partial x^2} - v\frac{\partial C}{\partial x} \tag{16.24}$$

The solution of Eq. (16.24) depends upon the knowledge of the relationship between adsorbed concentrations, S_s, and the solution concentration, C. Adsorption or exchange reactions perceived as instantaneous are described by equilibrium isotherms $S_s(C)$, which can be of the mass action, linear, Freundlich, Langmuir, or any other functional form (Nielsen et al., 1986). Besides adsorption, the reactive process such as first-order degradation and zero-order production can also be taken into account during miscible displacement process. Therefore, the comprehensive CDE for one-dimensional transport of reactive solutes, subject to adsorption, first-order degradation, and zero-order production, in a homogeneous soil, is written as:

$$\frac{\partial}{\partial t}(\theta C_r + \rho_b S_s) = \frac{\partial}{\partial x}\left(\theta D \frac{\partial C_r}{\partial x} - vC\right) - \theta \mu_\ell C_r - \rho_b \mu_s S + \theta \gamma_\ell(x) + \rho b \gamma_s(x) \tag{16.25}$$

where C_r is the volume-averaged or resident concentration of liquid phase (ML^{-3}), S_s is the concentration of the adsorbed phase (MM^{-1}), v is the volumetric water flux density (LT^{-1}), μ_l and μ_s are first-order decay coefficients for degradation of the solute in the liquid and adsorbed phases respectively (T^{-1}), γ_1 ($ML^{-3}T^{-1}$), and γ_s ($MM^{-1}\ T^{-1}$) are zero-order production terms for the liquid and adsorbed phases, D, θ, ρ_b, x, and t are the same as defined above. Assuming reversible equilibrium adsorption [Eq. (16.16)] and steady state flow in a homogeneous soil, Eq. (16.25) is modified to:

$$R\frac{\partial C_r}{\partial t} = D\frac{\partial^2 C_r}{\partial x^2} - v\frac{\partial C_r}{\partial x} - \mu C_r + \gamma(x) \tag{16.26}$$

where μ and γ are combined first- and zero-order rate coefficients

$$\mu = \mu_\ell + \frac{\rho_b K_D}{\theta} \tag{16.27}$$

$$\gamma(x) = \gamma_\ell(x) + \frac{\rho_b \gamma_s(x)}{\theta} \tag{16.28}$$

16.10 SORPTION PHENOMENON

Adsorption is a process where ions or molecules are attached to the surfaces of soil solids. This results in a higher concentration of solute at the surface of solid phase than in the bulk solution. The opposite of adsorption is anion exclusion where concentration in a soil solution is higher than the solid phase. Sorption and exclusion processes are important in modifying the movement of chemicals through a soil domain. The plot between amount adsorbed and the amount in solution is known as the adsorption isotherm (Fig. 16.6). The forces active at soil-water interface and at molecular level are electrical and are the same at both levels. These forces vary as the reciprocal of the separation distance raised to a power. Equilibrium sorption (Fig. 16.6) of organic molecules is dominated by the organic fraction of soil.

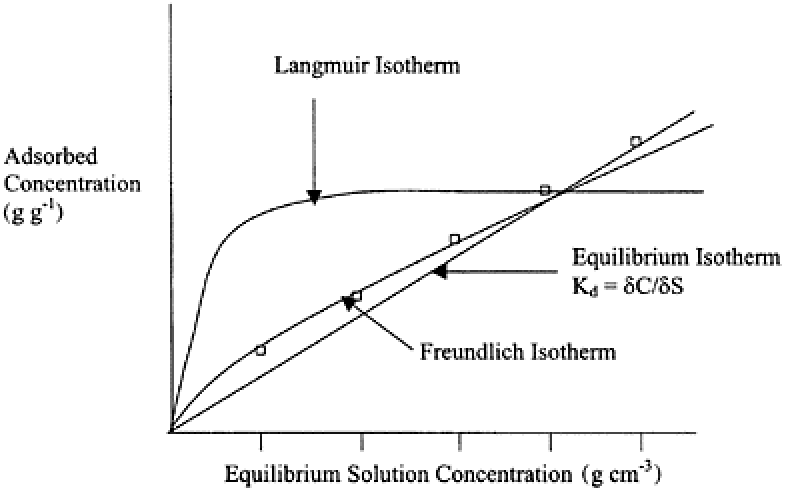

FIGURE 16.6 A schematic of adsorption isotherms. (Modified from July et al., 1994)

To account for this effect, value of K_D [Eq. (16.15)] is divided by soil organic carbon content (SOC) as below:

$$K_D = SOC * foc \tag{16.29}$$

The Freundlich adsorption model is given as $S_s = K_D C_l^n$, where n is close to 1 (Fig. 16.6). The Freundlich model is based on the assumption that there is no limiting concentration of adsorbate as solution concentration is increased without limit. This is unrealistic because available surfaces in soil domain are limited for adsorption to occur. The Langmuir adsorption model was developed from kinetics of gas adsorption on solid surfaces and has a sound conceptual basis. The model assumes that the energy of adsorption is constant and independent of surface coverage, the adsorbed molecules do not interact with each other, and the maximum possible adsorption is that of a complete monolayer (Fig. 16.6). The equilibrium adsorption (S_s) by Langmuir model is as follows:

$$S_s = \frac{aQC_l}{1 + aC_l} \tag{16.30}$$

where a is the ratio of adsorption rate constant, Q is the total number of available adsorption sites, and C_l is the solute concentration in solution. Several sorption models are available in literature, some are derived from the adsorption of gases by solids while others are either empirical or kinetic.

Based upon multireaction approach, Selim (1992) proposed a model that involves three types of sites during sorption. The first type of site is equilibrium (S_{se}), where equilibrium between the sorbed and solution phases is established quickly. The second type of sites is kinetic, S_{sk}, where adsorption is considered time dependent, and the third type-site is subjected to irreversible retention S_{sir}. Total amount of sorption can be described by the following relationship

$$S_s=S_{se}+S_{sk}+S_{sir} \tag{16.31}$$

Some of the equilibrium and kinetic sorption relationships are presented in Table 16.3.

16.11 EQUILIBRIUM ANION EXCLUSION MODEL

Certain anions interact with the negatively charged solid surfaces of the soil (such as clay or ionizable organic matter) and are excluded from the liquid region adjacent to the soil particle surfaces. This phenomenon is known as anion exclusion or negative adsorption. Eq. (16.17) represents the anion exclusion phenomenon for $R<1$. In the presence of a soil solution, the negative charge extends from the surfaces of particles into the solution and forms diffuse double layer (Bolt, 1979). The existence of the negative charge causes repulsion of anions from this region. The resulting concentration gradient reduces the concentration of anion at the soil surface to zero, which increases exponentially with distance and at the limit of diffuse double layer becomes equal to the concentration of bulk solution (Bolt, 1979). Assuming that effective exclusion volume (θ_{ex}) expressed as volumetric moisture content is evenly distributed over the particle surface, the one-dimensional transport of an anionic solute exhibiting anion exclusion can be described as follows (Bresler, 1973; James and Rubin, 1986)

$$(\theta-\theta_{ex})\frac{\partial C}{\partial t}=D\frac{\partial^2 C}{\partial x^2}-q\frac{\partial C}{\partial x} \tag{16.32}$$

The observed concentration (C) is less than the concentration of bulk solution (C_0) because of the exclusion volume, which does not contain ions. This interrelationship between C and C_0 can be expressed as follows:

$$C=C_0\left[1-\frac{\theta_{ex}}{\theta}\right] \tag{16.33}$$

TABLE 16.3 Equilibrium and Kinetic Models for Sorption in Soils[a]

Model	Formulation
EQUILIBRIUM TYPE	
Linear	$S_{se}=K_DC_l$
Freundlich	$S_{se}=K_DC_l^n$
General Freundlich	$S_s/S_{smax}=[\omega C/(1+\omega C)]\beta$
Rothmund-Kornfeld ion exchange	$S_{si}/S_{sT}=K_D(C_i/C_T)^n$

Langmuir	$S_s/S_{smax}=(\omega C)^{\beta}+\omega C)$
General Langmuir-Freundlich	$S_s/S_{smax}=(\omega C)^{\beta}/(1+\omega C)^{\beta}$
Langmuir with sigmoidicity	$S_s/S_{smax}=(\omega C)/(1+\omega C+\omega/C)$
KINETIC TYPE	
First order	$\partial S_s/\partial t=K_D(\theta/\rho b)(C_l-KD_1S_s)$
*n*th order	$\partial S_s/\partial t = K_D(\theta/\rho_b)(C_l^n - K_{D1}S_s)$
Irreversible (sink/source)	$\partial S_s/\partial t=K_D(\theta/\rho_b)(C-C_p)$
Second-order irreversible	$\partial S_s/dt=K_D(\theta/\rho b)C(S_{smax}-S_s)$
Langmuir kinetic	$\partial S_s/\partial t=KD(\theta/\rho b)C(S_{smax}-S_s)-K_DS_s$
Elovich	$\partial S_s/\partial t=A\ exp(-BS_s)$
Power	$\partial S_s/\partial t = K_D(\theta/\rho_b)C^n S_s^m$
Mass transfer	$\partial S_s/\partial t=K_D(\theta/\rho_b)(C-C^*)$

[a] Where *k, A, B, n m,* S_s, S_{smax}, C^*, C_p, and ω are adjustable model parameters.
Source: Modified from Selim and Amacher, 1997.

If the sufficient volume of input solution (concentration=C_0) infiltrates in a soil column for a long duration, the excluded water content can be calculated by using Eq. (16.34) (Bond et al., 1982)

$$\theta_{ex} = \theta\left[1 - \frac{C}{C_0}\right] \qquad (16.34)$$

The C in the soil profile is always lower than C_0 when anion exclusion is occurring. The anion exclusion also increases the average velocity of travel of anions in the soil profile. By excluding the anions from the diffuse double layer where water is either moving slowly or is immobile, the rate of transport is greater than given by q/θ. Bolt (1979) assumed anion exclusion to be evenly distributed over the soil surface of thickness d_{ex}.

$$d_{ex} = \frac{Q}{\sqrt{\beta N}} - \delta \qquad (16.35)$$

where β is a constant (1.06×10^{19} mkeq^{-1} at 25°C), N is the total normality of bulk solution (keq m^{-3}), Q is a factor for ionic composition of bulk solution (m^{-1}), and δ a correction term. The specific surface area (A_r) can be calculated from exclusion volume and bulk density (ρ_b; Mg m^{-3}) as follows

$$A_r = \frac{\theta_{ex}}{d_{ex}\rho_b} * 10^{-6} \qquad (16.36)$$

16.12 NONEQUILIBRIUM TRANSPORT

The application of Eq. (16.24) or (16.26) to transport through laboratory soil columns or in fields having relatively uniform soils involving nonreactive or weakly reactive solutes was found to be fairly successful (Biggar and Nielsen, 1976; Jaynes, 1991; Ellsworth et al., 1996; Shukla et al., 2003). The BTCs for these tracers are symmetrical and mass recoveries are relatively high (Fig. 16.7). However, for strongly adsorbed chemicals and aggregated soils these equations do not perform very well (van Genuchten and Wierenga, 1976; Nkedi-Kizza et al., 1984).

During solute transport in heterogeneous soils, the assumption of local equilibrium implies instantaneous interchange of mass, large residence time sufficient to make concentration gradients negligible, and high degrees of interactions between macroscopic transport properties and microscopic soil physical properties. Some of the macroscopic transport properties are water flux, apparent dispersion, and moisture content, and microscopic properties are aggregate size, exchange, pore geometry. The microscopic properties impose a rate limiting effect on solute transport through heterogeneous soils and deviations from local equilibrium conditions are observed. The mass recoveries, for these asymmetrical and nonsigmoidal concentration distributions or BTCs, are less and the BTCs have a long tail (Fig. 16.7). Such a deviation is caused by a number of physical and chemical nonequilibrium processes. The physical nonequilibrium is caused by a heterogeneous flow regime and a chemical nonequilibrium by the kinetic adsorption. This paves the way for the examination of diffusion controlled or chemically controlled kinetic rate reactions or both of the form $\partial S/\partial t=f(S_s, C)$. The following sections will examine briefly the nonequilibrium processes arising out of physical or chemical nonequilibrium.

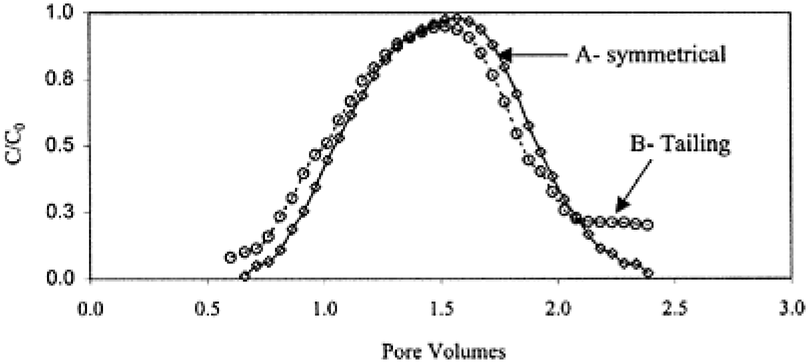

FIGURE 16.7 Schematic of equilibrium and nonequilibrium transport of a tracer through laboratory soil columns, the ETC "A" is symmetrical and mass recoveries are higher than a asymmetrical ETC "B".

16.13 TWO-REGION NONEQUILIBRIUM TRANSPORT MODEL

There are several factors responsible for physical nonequilibrium conditions occurring in a soil system during solute transport. Some of them are: (i) heterogeneity of pore size distribution or aggregation; (ii) heterogeneous diffusion into the Neurst film of water surrounding soil particles than soil bulk solution. Physical nonequilibrium is represented by a two-region (dual porosity) type formation. In this case, the medium is assumed to contain two distinct mobile (flowing) and immobile (stagnant) liquid regions. The simplest explanation of a two region mobile and immobile formation is the water inside an aggregated soil. All the intraaggregate water held within an aggregate is immobile and the interaggregate (between aggregates) water is mobile. The water flowing around dry aggregates imbibes them and solute entry inside aggregate is by convection. For moist aggregate, solute entry is governed by diffusion. However, there must be a concentration gradient from outside to the inside of an aggregate, and a first-order process can adequately describe the mass transfer between the two regions. In a two-region model, convective diffusion transport is assumed to take place in the mobile region while transfer of solutes into and out of mobile region is assumed to be diffusion controlled. One-dimensional unsaturated flow of conservative nonsorbing solute in a soil is given as follows (Coats and Smith, 1964):

$$\theta_m \frac{\partial C_m}{\partial t} + \theta_{im} \frac{\partial C_{im}}{\partial t} = \theta_m D_m \frac{\partial^2 C}{\partial x^2} - \theta_m v_m \frac{\partial C_m}{\partial x} \tag{16.37}$$

$$\theta_{im} \frac{\partial C_{im}}{\partial t} = \alpha (C_m - C_{im}) \tag{16.38}$$

where t is time *(T)*; C_m and C_{im} are the solute concentrations in the mobile and immobile liquid phases (ML^{-3}) with corresponding volumetric moisture contents θ_m and θ_{im} (L^3/L^3) respectively; D_m is apparent diffusion coefficient of mobile liquid phase (L^2T^{-1}); x is the distance from the inflow boundary in the direction of flow *(L)*; v_m is the average mobile pore water velocity in (LT$-^{1}$); and *a* is the first order rate coefficient (T^{-1}).

In Eqs. (16.37) and (16.38) as the ratio of mobile water fraction (θ_m) to total moisture content (θ) increases (i.e., θ_m increases), more and more of the wetted pore space is included in the transport, which causes greater and more complete mixing, and the ETC shifts further to the right. At the extreme end, the $\theta_m=\theta$, where the above equation reduces to one-dimensional CDE [Eq. (16.23)]. The parameter α, which has the dimensions of T^{-1}, can vary from 0 to ∞. A zero value of a indicates no mixing between mobile and immobile water fractions. Therefore, the term on left-hand side of Eq. (16.38) equals zero and Eq. (16.37) reduces to one-dimensional CDE, similar to Eq. (16.23) but with total moisture content of θ_m. When $a=\infty$, the two concentrations mix instantaneously and $C_m=C_{im}$. In this case Eq. (16.37) reduces to Eq. (16.23).

One-dimensional solute transport for an exchanging solute during steady-state flow through a homogeneous porous medium, where the liquid phase is presumed to consist of a mobile and immobile region and includes a Freundlich-type equilibrium adsorption-desorption processes (van Genuchten and Wierenga, 1976) can be described by a two-region model as follows:

$$\theta_m \frac{\partial C_m}{\partial t} + f\rho_b \frac{\partial S_{sm}}{\partial t} + \theta_{im} \frac{\partial C_{im}}{\partial t} + (1-f)\rho_b \frac{\partial S_{sim}}{\partial t} = \theta_m D_m \frac{\partial^2 C}{\partial x^2} - \theta_m v_m \frac{\partial C_m}{\partial x} \tag{16.39}$$

and

$$\theta_{im} \frac{\partial C_{im}}{\partial t} + (1-f)\rho_b \frac{\partial S_{sim}}{\partial t} = \alpha(C_m - C_{im}) \tag{16.40}$$

where S_{sm} and S_{sim} are concentration of adsorbed phase in mobile and immobile phase respectively (MM^{-1}); R_m and R_{im} are retardation factors accounting for equilibrium type adsorption processes in mobile and immobile regions, respectively; and parameter/represents the mass fraction of solid phase that is in direct contact with the mobile liquid phase. If the exchange process in both the dynamic (S_{sm}) and stagnant (S_{sim}) region is assumed to be instantaneous, linear and reversible process (van Genuchten, 1981) then,

$$S_{sm}=K_D C_m \text{ and } S_{sim}=K_D C_{im} \tag{16.41}$$

and the total adsorption can be represented by

$$S_s=fS_{sm}+(1-f)S_{sim} \tag{16.42}$$

For equilibrium adsorption, transferring these into Eqs. (16.39) and (16.40) results in following set of equations

$$(\theta_m + \rho_b f k)\frac{\partial C_m}{\partial t} + [\theta_{im} + (1-f)\rho_b k]\frac{\partial C_{im}}{\partial t} = \theta_m D_m \frac{\partial^2 C_m}{\partial x^2} - \theta_m v_m \frac{\partial C_m}{\partial x} \tag{16.43}$$

$$[\theta_{im} + (1-f)\rho_b K_D]\frac{\partial C_{im}}{\partial t} = \alpha(C_m - C_{im}) \tag{16.44}$$

16.14 TWO-REGION ANION EXCLUSION MODEL

The two-region anion exclusion model divides the total soil-water phase into two compartments, (i) mobile water and (ii) immobile water, and anion exclusion is assumed to take place in the immobile region (van Genuchten, 1981). This assumption is analogous to the assumptions made by Krupp et al. (1972), as anion exclusion takes place in the smaller pores inside the dense aggregate or in the immobile water along the pore wall. An equivalent exclusion distance (d_{ex}) exists near the pore wall where concentration remains zero. Therefore, specific exclusion volume (V_{ex}; cm^3 water g^{-1} of soil) is related to specific surface area (A_m; $cm^2\ g^{-1}$) and d_{ex} as follows:

$$V_{ex}=d_{ex}A_m \tag{16.45}$$

The θ_{ex} is obtained by multiplying Eq. (45) by soil bulk density (ρ_b)

$$\theta_{ex}=V_{ex\rho b} \tag{16.46}$$

The part of liquid phase unaffected by anion exclusion (θ_a) can be calculated as follows:

$$\theta_a=\theta_{im}-\theta_{ex} \tag{16.47}$$

Using Eq. (16.47), the following physical nonequilibrium equation representing the anion exclusion process is obtained (van Genuchten, 1981)

$$\theta_m\frac{\partial C_m}{\partial t}+\theta_a\frac{\partial C_a}{\partial t}=\theta_m D\frac{\partial^2 C_m}{\partial x^2}-\theta_m v_m\frac{\partial C_m}{\partial x} \tag{16:48}$$

$$\theta_a\frac{\partial C_a}{\partial t}=\alpha(C_m-C_a) \tag{16.49}$$

where C_a is concentration in the part of immobile zone unaffected by exclusion. The model described above assumes anion exclusion taking place inside the immobile water zone. Therefore, convective transport in mobile zone remains unaffected by the exclusion process and C_m never exceeds input concentration C_0 (van Genuchten, 1981).

16.15 TWO-SITE NONEQUILIBRIUM TRANSPORT MODEL

Considering that the solid phase of soil is made up of various constituents (i.e., soil minerals, organic matter, aluminum, and iron oxides), and chemical react with these different constituents at different rates and intensities. Selim et al. (1976) and Cameron and Klute (1997) proposed a two-site chemical nonequilibrium model where adsorption term consists of two components, equilibrium adsorption, and first-order kinetics. The sorption or exchange sites in this model are assumed to have instantaneous adsorption (type-1 sites) and time-dependent kinetic adsorption (type-2 sites). At equilibrium, adsorption on both types of sorption sites is described by the following linear equations:

$$S_{s1}=K_{De}C=FK_DC \tag{16.50}$$

$$S_{s2}=K_{Dk}C=(1-F)K_DC \tag{16.51}$$

where subscript *"e"* refers to type 1 or equilibrium site and subscript *"k"* refers to type 2 or kinetic sites, respectively, and F is the fraction of all sites occupied by type 1 sorption sites. Total adsorption at equilibrium is

$$S_s=S_{se}+S_{sk} \tag{16.52}$$

Because type 1 sites are always at equilibrium therefore,

$$\frac{\partial S_{se}}{\partial t} = FK_D \frac{\partial C}{\partial t} \qquad (16.53)$$

The adsorption rate for type 2 kinetic nonequilibrium sites can be given by a linear and reversible first order equation of following form

$$\frac{\partial S_{sk}}{\partial t} = \alpha[(1 - F)K_D C - S_{sk}] \qquad (16.54)$$

where α is the first order rate coefficient. Combining above equations with Eq. (16.14) lead to following formulation (van Genuchten, 1981; Nkedi-Kizza et al., 1984):

$$\left(1 + \frac{F\rho_b K_D}{\theta}\right)\frac{\partial C}{\partial t} + \frac{\rho_b}{\theta}\frac{\partial S_{sk}}{\partial t} = D\frac{\partial^2 C}{\partial x^2} - v\frac{\partial C}{\partial x} \qquad (16.55)$$

$$\frac{\partial S_{sk}}{\partial t} = \alpha[(1 - F)K_D C - S_{sk}] \qquad (16.56)$$

16.16 INITIAL AND BOUNDARY CONDITIONS FOR STEP INPUT EXPERIMENTS

The analytical solutions of Eqs. (16.23), (16.24), (16.25), (16.43), (16.44), (16.48), (16.49), (16.55), and (16.56) are available for a large number of initial and boundary conditions for both finite and semi-infinite systems for both step and pulse type solute application (van Genuchten 1981, van Genuchten and Alves, 1982). This section briefly describes some of the initial and boundary conditions required for solving solute transport equations. The most common initial condition for any soil is:

$$C(x, 0)=C_i \qquad (16.57)$$

At the upper boundary of the soil surface or (or inflow into the soil column; i.e. at $x=0$), two different boundary conditions can be considered. The first type or constant concentration boundary condition is of the form as follows:

$$C(0, t)=C_0 \qquad (16.58)$$

For column displacement experiments, where chemical is applied at a constant rate, the boundary condition (16.58) leads to mass balance errors, which become quite significant for large values of *(D/v)* (van Genuchten, 1981, Parker and van Genuchten, 1984). The other boundary condition is a third type, or constant flux type, that leads to the conservation of mass inside the soil column provided dispersion outside the soil can be ignored is given as follows: